Simulating Free Surface Flows with SPH

J. J. MONAGHAN

Department of Mathematics, Monash University, Clayton Victoria 3168, Australia

The SPH (smoothed particle hydrodynamics) method is extended to deal with free surface incompressible flows. The method is easy to use, and examples will be given of its application to a breaking dam, a bore, the simulation of a wave maker, and the propagation of waves towards a beach. Arbitrary moving boundaries can be included by modelling the boundaries by particles which repel the fluid particles. The method is explicit, and the time steps are therefore much shorter than required by other less flexible methods, but it is robust and easy to program. © 1994 Academic Press, Inc.

1. INTRODUCTION

Free surface flows in hydrodynamics are of great industrial and environmental importance but they are difficult to simulate because boundary conditions are required on an arbitrarily moving surface. The MAC method [5], which uses particles to define the surface and finite differences to solve the hydrodynamic equations, is the most flexible and robust of the available numerical methods. It has been applied to a wide variety of problems (for references see [4]), including waterfalls, breaking dams, and two-fluid instabilities, and it has been extended to deal with moving boundaries [16] and simplified [6], but it remains complicated to program.

In this paper we consider the application of the particle method SPH (smoothed particle hydrodynamics) to free surface problems. SPH is a Lagrangian particle method which does not require a grid and can be used to simulate a compressible fluid moving arbitrarily in three dimensions. It is robust and simple to program. There have been numerous applications in astrophysics ([8, 3]; for reviews see [10, 12, 2]), where complex gas dynamics involving supersonic velocities, radiation, nuclear reactions, and the high speed collision of metals have been successfully treated. However, it is not clear that the method can be extended to the simulation of incompressible fluids, not is it clear that boundaries can be incorporated easily. The purpose of this paper is to show that such an extension is possible.

There are at least two ways that SPH might be extended to incompressible or nearly incompressible flow. The first of these is to work directly with the constraint of constant density. It is possible to include these constraints easily in the SPH formalism by using the Gibbs–Appell equations [15] which are generalized versions of Gauss' principle of least constraint. Unfortunately, the resulting equations are cumbersome, and it has not been possible to solve them efficiently without further approximations.

The second approach, and the one we use here, is based on the observation that real fluids such as water are compressible, but with a speed of sound which is very much greater than the speed of bulk flow. The momentum equation shows that the variation in density $\delta\rho$ is given by

$$\frac{\delta\rho}{\rho} = \frac{vL}{c^2\tau}$$

where L is a typical length scale of the flow, τ is a typical time scale, and v is a typical velocity. For the problems we are considering, $v = L/\tau$, so that the relative fluctuation in density is proportional to M^2, where M is the Mach number. For fluids like water, with sound speed $\sim 10^3$ ms^{-1}, the Mach number is extremely small, and it is customary to approximate the fluid by an artificial fluid which is exactly incompressible. The approach here is different. The real fluid is approximated by an artificial fluid which is more compressible than the real fluid. The artificial fluid has a speed of sound which is still much larger than the speed of bulk flow and therefore has very small density fluctuations.

The standard SPH formulation of fluid dynamics can then be taken over largely unchanged. The price paid is that, if density fluctuations are to be $\sim 1\%$, M must be ~ 10 and the Courant condition then requires ~ 10 times as many steps as in other methods. However, these other methods often require several iterations for each step (MAC is an example), and the disparity in work is therefore not as great as it might seem at first sight. To offset the many time steps we also have the advantage of great ease of use. It is, for example, easy to convert the programs to deal with more materials and different boundaries.

Apart from showing how SPH may be used for free sur-

face problems we show how boundaries may be modelled very simply by using boundary particles which impose forces on the fluid [17, 18]. This idea is based on the fact that real boundaries are produced by atoms or molecules which exert forces on the fluid. The boundary condition that the velocity normal to the boundary vanishes at the boundary can therefore be replaced by a boundary force in the momentum equation. The real boundary force has the short range of atomic dimensions, but it can be approximated by an artificial force with a range close to the resolution length of the calculation. If a viscous boundary condition is required we include the boundary particles in the calculation of the viscous stress.

The boundary particles can be set up to follow any fixed or moving boundary. As an example, the simulation of a complete wave generator with the moving parts, fluid, and the beach will be described.

It is interesting, and possibly useful, that the SPH formulation with boundary forces leads to a very simple Hamiltonian formulation of fluid dynamics.

2. THE SPH EQUATIONS

The SPH equations for a compressible gas are described in detail by Monaghan [12]. They are obtained from the continuum equations of fluid dynamics by interpolating from a set of points which may be disordered. The interpolation is based on the theory of integral interpolants using interpolation kernels which approximate a delta function. The interpolants are analytic funcions which can be differentiated without the use of grids. If the points are fixed in position the equations are identical to finite difference equations with different forms depending on the interpolation kernel.

The SPH equations describe the motion of the interpolating points which can be thought of as particles. Each particle carries a mass m, a velocity v, and other properties depending on the problem.

The momentum equation for particle a becomes

$$\frac{dv_a}{dt} = -\sum_b m_b \left(\frac{P_a}{\rho_a^2} + \frac{P_b}{\rho_b^2} + \Pi_{ab} \right) \nabla_a W_{ab} + F_a, \quad (2.1)$$

where the summation is over all particles other than particle a (although in practice only near neighbours contribute), P is the pressure, and ρ is the density, Π_{ab} produces a shear and bulk viscosity, F_a is a body force (for the problems considered here this is gravity), W_{ab} is the interpolating kernel, and ∇_a denotes the gradient of the kernel taken with respect to the coordinates of particle a. The terms involving the pressure are derived from the pressure gradient. They are written in symmetrized form to conserve linear and angular momentum when the kernel is symmetric.

In this paper we use the spline based kernel [13, 12]. The kernel depends on a length h which determines the resolution (see (2.7)). For separations $> 2h$ the kernel vanishes so that the summations only involve near neighbours. Typically h is $>$ the initial particle separation. It is possible to have a different resolution length for each particle, but this should not be necessary for incompressible flow.

The viscous term Π_{ab} has the general form

$$\Pi_{ab} = \begin{cases} \dfrac{-\alpha \bar{c}_{ab} \mu_{ab} + \beta \mu_{ab}^2}{\bar{\rho}_{ab}}; & v_{ab} \cdot r_{ab} < 0 \\ 0; & v_{ab} \cdot r_{ab} > 0, \end{cases}$$

where

$$\mu_{ab} = \frac{h v_{ab} \cdot r_{ab}}{r_{ab}^2 + \eta^2}.$$

In these expressions the notation $A_{ab} = A_a - A_b$, and $\bar{A}_{ab} = (A_a + A_b)/2$ has been used, and c is the speed of sound. Because of its symmetry the viscous term conserves linear and angular momentum. The viscosity vanishes for rigid rotation. For the problems described here we take β as zero. The term involving α introduces both shear and bulk viscosity into incompressible flow. In the present case, with negligible changes in the density, the viscosity is almost entirely shear viscosity with a viscosity coefficient approximately αhc. In most of the calculations we take $\alpha = 0.01$.

The normal practice in SPH calculations is to find the smoothed density by summing over the particles according to

$$\rho = \sum_b m_b W_{ab}. \quad (2.2)$$

However, if (2.2) is used for fluids like water, where the density falls discontinuously to zero at the surface, the density will be smoothed over the length $2h$ and surface particles will have a low density. The equation of state will then introduce incorrect pressures and degrade the calculation. It is therefore preferable to depart from normal practice and approximate the rate of change of the density. All particles are then assigned the same initial density which only changes when particles are in relative motion.

Writing the continuity equation in the form

$$\frac{d\rho}{dt} = -\nabla \cdot (\rho v) + v \cdot \nabla \rho,$$

and using SPH particle interpolants for the right-hand side, the rate of change of the density of particle a becomes

$$\frac{d\rho_a}{dt} = \sum_b m_b (v_a - v_b) \cdot \nabla_a W_{ab}. \quad (2.3)$$

There is also a computational advantage in using (2.3) since all rates of change can be calculated in one pass over the particles, whereas with (2.2), there is one pass to calculate the density, then another pass to calculate the rate of change of velocity.

The thermal energy per unit mass changes according to

$$\frac{du_a}{dt} = \frac{1}{2} \sum_b m_b \left(\frac{P_a}{\rho_a^2} + \frac{P_b}{\rho_b^2} + \Pi_{ab} \right) \mathbf{v}_{ab} \cdot \nabla_a W_{ab}. \quad (2.4)$$

The rate of change of particle position is

$$\frac{d\mathbf{r}_a}{dt} = \mathbf{v}_a, \quad (2.5)$$

but it proves important for the free surface problems to use the XSPH variant which involves adding the following correction to the right-hand side of (2.5),

$$\Delta_a = \varepsilon \sum_b \frac{m_b (\mathbf{v}_b - \mathbf{v}_a)}{\bar{\rho}_{ab}} W_{ab}. \quad (2.6)$$

This correction to the velocity keeps the particles more orderly and, in high speed flow, prevents the penetration of one fluid by another [11].

In this paper we choose $\varepsilon = 0.5$. For consistency the velocity used in the continuity equation should be the velocity used for stepping the particles. This is not necessary for relatively placid flows (such as the breaking dam), but it was found necessary for the simulated wave maker. Note that each particle has effectively two velocities. One of these, $\mathbf{v}$, comes from the momentum equation, while the other is the corrected velocity used for moving the particles.

For the reader unfamiliar with the SPH equations they may be interpreted conveniently using a gaussian kernel. In two dimensions the gaussian kernel has the form

$$W_{ab} = \exp(-(\mathbf{r}_a - \mathbf{r}_b)^2/h^2)/(\pi h^2), \quad (2.7)$$

and the contribution of particle b to the acceleration of particle a is easily seen to be a symmetric central force. From this fact it follows that the method conserves linear and angular momentum. In the same way it can be seen that the density of particle a increases when particle b is moving towards it.

3. THE EQUATION OF STATE

As remarked earlier, the density variation in fluid flow is $\propto M^2$, where M is the Mach number. Batchelor [1] gives an equation of state for water which describes sound waves accurately. This equation of state, modified to give a smaller

speed of sound, is suitable for the simulation of the bulk flow of the fluid. The equation of state has the form

$$P = B \left(\left(\frac{\rho}{\rho_0} \right)^\gamma - 1 \right), \quad (3.1)$$

with $\gamma = 7$. This equation of state is the first one that I tried and no attempt has yet been made to fine-tune the method by choosing a different equation of state. The choice of B determines the speed of sound. For example, when a dam of height H collapses, an approximate upper bound to the speed v of the water is given by

$$v^2 = 2gH \quad (3.2)$$

and the coefficient B in the equation of state should be taken as

$$B = \frac{200gH}{\rho\gamma} \quad (3.3)$$

with a speed of sound c approximately $\sqrt{200gH}$ and $M \sim 0.1$. Numerical experiments confirm that the density variations are consistent with this estimate. In a similar way an equation of state can be set up for any flow problem. Other examples will be given later.

4. BOUNDARY CONDITIONS

Most of the calculations to be described here were made with boundary particles which exert central forces on fluid particles. The form for the force was guided by the known forces between molecules. For a boundary and fluid particle separated by a distance r the force per unit mass $f(r)$ has the Lennard-Jones form

$$f(r) = D \left(\left(\frac{r_0}{r} \right)^{p_1} - \left(\frac{r_0}{r} \right)^{p_2} \right) \frac{\mathbf{r}}{r^2}, \quad (4.1)$$

but is set to zero if $r > r_0$ so that the force is purely repulsive. The constants p_1 and p_2 must satisfy the condition $p_1 > p_2$ and for most of the simulations $p_1 = 4$ and $p_2 = 2$. Similar results were found with $p_1 = 12$ and $p_2 = 6$. There is some evidence from numerical calculations that there might be an advantage in allowing the force to attract at large distances, or to go to zero smoothly, but these possibilities have not been explored.

The length scale r_0 is taken to be the initial spacing between the particles, and the coefficient D (with dimensions v^2) was chosen by considering the physical configuration. For problems involving dams, bores, or weirs with fluid of depth H, we take $D = 5gH$, where H is the depth of the water, but $D = 10gH$ or $D = gH$ give similar results.

Peskin [17] constructed boundary forces by assuming that there was a concentrated force at the boundary which could be described by a delta function. This idea can be implemented in different ways according to the way the delta function is approximated. However, in the calculations described here, the use of forces based on known molecular forces worked better than forces based on approximations of the delta function.

Apart from preventing penetration and therefore ensuring that the normal component of the velocity vanishes, boundary particles may be required to correctly produce no-slip conditions. Where this is required the boundary particles are included in the calculation of the viscous terms in the momentum equation.

5. IMPLEMENTATION

For the two-dimensional calculations described here the particles can be set up initially on a cartesian lattice, or preferably, on an hexagonal lattice. The mass of particle b is given by $m_b = \rho_b \, \Delta A$, where ΔA is the area per particle. Particles that extend beyond boundaries are removed. Some care needs to be exercised near sloping or curved boundaries because some particles from the lattice may end up very close to the boundary particles and experience a huge boundary force. In such cases the initializing routine should ensure that no fluid particle is too close to the boundary particles.

The particles are assigned an initial density $10^3 \, \text{kg/m}^3$ which in gravity flows may need to be adjusted to give the correct hydrostatic pressure when the pressure is calculated from the equation of state. For example, when the gravity acts in the negative y direction, the density is given by

$$\rho = \rho_0 \left(1 + \frac{\rho_0 \, g(H - y)}{B} \right)^{1/\gamma}, \qquad (5.1)$$

where H is the depth.

Even with adjustments to the density to ensure that the initial state is near equilibrium the system may still have substantial unbalanced forces. To settle the system down to an equilibrium state a damping term, $-\Gamma v$, was introduced into the momentum equations, and the damping was continued until the kinetic energy was very low, after which $\Gamma = 0$. The system was then activated by setting up the perturbations or moving boundaries required to initiate the motion to be studied.

The summations can be evaluated efficiently using link lists to access neighbouring particles [13]. The link list uses a grid of bookkeeping cells with size $2h$. Only particles in neighbouring cells can then contribute to the properties of particles in a given cell.

Time stepping is carried out using a predictor–corrector scheme. For an equation of the form

$$\frac{dv}{dt} = -\Gamma v + F \qquad (5.1)$$

the predictor step predicts to the midpoint so that, with time step δt, the midpoint v is

$$v^{n+1/2} = \frac{v^n + 0.5 \delta t \, F^n}{1 + 0.5 \Gamma \, \delta t} \qquad (5.2)$$

with corrector step

$$v^{n+1/2} = \frac{v^n + 0.5 \, \delta t \, F^{n+1/2}}{1 + 0.5 \Gamma \, \delta t}. \qquad (5.3)$$

In each step the damping term is treated implicitly. The value of $\mathbf{v}$ at the end of the step is then

$$v^{n+1} = 2v^{n+1/2} - v^n. \qquad (5.4)$$

To speed up the calculations the predictor step uses the value of F at the previous midpoint. The errors are still of $O(\delta t^3)$. The time step is largely controlled by the Courant condition, but we use the general SPH time step control [7] which includes the effect of viscosity and body forces. The value of $\Gamma \, \delta t$ was typically 0.05.

6. THE EVOLUTION OF AN ELLIPTICAL DROP

A simple test of the SPH formulation is the flow of an elliptical drop in two dimensions when the initial velocity field is linear in the coordinates. The condition that the drop remains elliptical with time varying axes a and b is that

$$v_x = \frac{x}{a}\frac{da}{dt}, \qquad v_y = \frac{y}{b}\frac{db}{dt}, \qquad (6.1)$$

where, for example, v_x is the x component of velocity. The condition that the fluid remains incompressible is that ab is constant which also follows from the vanishing of $\nabla \cdot \mathbf{v}$.

TABLE I

SPH and Theoretical (Based on (6.2), (6.3)) Values of b (Semi-Major Axis) of the Elliptical Drop

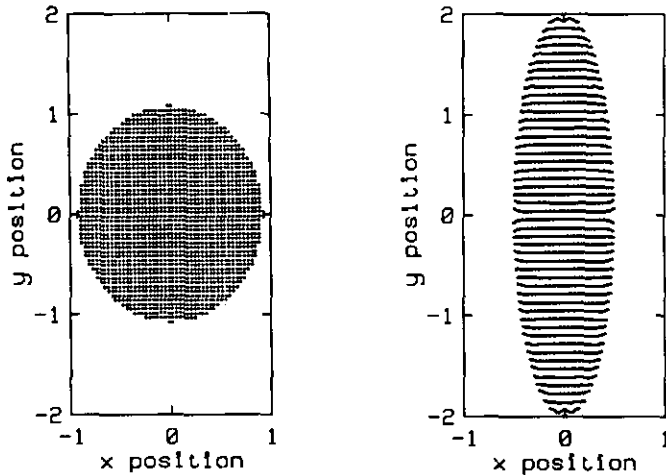| Time/s	Theory	SPH
0.0008	1.083	1.086
0.0038	1.44	1.44
0.0076	1.95	1.91

FIG. 1. Particle positions for the evolution of an elliptical drop as it evolves from a circle to a narrow ellipse. The initial speed is 141 m/s and the two frames are at 0.0008 s and 0.0082 s.

From the momentum equation and the condition that the pressure is constant on the elliptical surface, we deduce that

$$\frac{dA}{dt} = \frac{A^2(a^4 - \omega^4)}{a^4 + \omega^4},$$
(6.2)

where A is defined by

$$\frac{da}{dt} = -aA,$$
(6.3)

and ω is the initial value of ab.

These equations can be solved to high accuracy and the results compared with the SPH simulation. The initial velocity field was $(-100x, 100y)$ and the initial fluid configuration was a circle of radius 1 m. The pressure was computed using a coefficient that gave the normal pressure for water and a sound speed of 1400 m/s. In this case, as expected, the density fluctuations were $<1\%$. In Fig. 1 we show two fluid particle configurations from a simulation using 1884 particles. It is apparent that the particle configuration preserves a smooth outer boundary with no tendency to break up or become ragged. In Table I the run of the semi-major axis is shown. The errors in the calculation are $<2\%$.

7. BURSTING DAM

The simplified bursting dam has been simulated using MAC [5, 14] and the results are compared with the experiments of Martin and Noyce [9]. In the SPH calculation the boundary was simulated with the Lennard-Jones boundary force, 2910 particles were used for the simulation, and $\alpha = 0.01$. In this simulation boundary particles form the left-hand boundary, the base, and a small triangular obstacle.

In Fig. 2 the particle configurations for the collapsing dam are shown at representative times. The particles maintain an orderly configuration until they meet the obstacle when they simulate a splash. The appearance before the fluid meets the obstacle is very similar to the MAC simulations.

In Table II we compare the SPH results with the experimental results of Martin and Moyce [9]. The surge
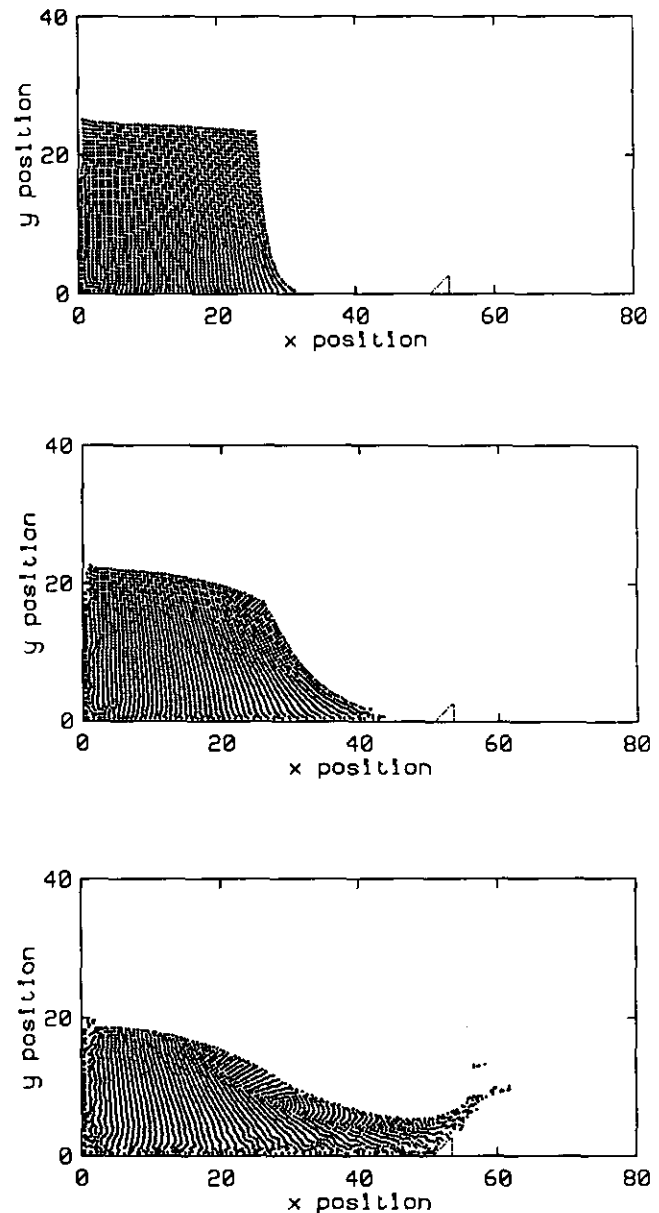

FIG. 2. The positions of 2910 water particles in the evolution of a column of fluid under gravity. Boundary particles form the boundary to the left, the base, and the triangular obstacle. The Lennard-Jones boundary force was used. Other details are given in the text.

TABLE II

Experimental and SPH Values of the Surge Front Z and
Height H of a Fluid Column Collapsing under Gravity

Time	H (exp)	H (SPH)	Z (exp)	Z (SPH)
0.71	0.90	0.90	1.33	1.56
1.39	0.76	0.75	2.25	2.50
2.10	0.57	0.56	3.22	3.75
3.20	0.32	0.37	4.80	5.00

Note. Units and further details are in the text.

front Z and height of the dam H are in units of H_0; the initial height of the dam (this is the case $n = 1$ of Martin and Noyce), and the time is in units of $\sqrt{H_0/g}$. Because the timing in the experiment has an error of ~ 0.1 the comparison of the results is only approximate. With this proviso the agreement is satisfactory. Note that the SPH values of Z exceed those of the experiment and suggest that the experimental results are affected by drag between the fluid and the bottom.

Close examination of Fig. 2 shows that the boundary does affect the particle configuration, but only within a distance of $\sim h$ of the boundary. For example, the first frame indicates that at the top left-hand corner of the fluid the boundary force has kept the fluid further away than at the base. This is because the hydrostatic pressure is smaller near the top than at the bottom. The error is, however, always $\sim h$ which is acceptable and equivalent to a slight perturbation to the wall. There is also an indication that the motion of particles moving near the horizontal boundary is perturbed by the particle barrier. When the Lennard-Jones boundary force was replaced by the gaussian force similar boundary effects were noted, but a careful study of the effects of different boundary forces has not been completed.

8. BORE

In Fig. 3 we show the formation of a bore. The fluid on the right is moving to the left with an initial velocity of 8.6 m/s and depth 10 m. Particles form the bottom and the left-hand wall. Several experiments were run with different initial conditions and different viscosities. If all the fluid is initially moving to the left, there is a surge up the wall and a splash which complicates the interpretation. It was found preferable to start with some fluid near the left boundary at rest and at height 20 m. The bore then rapidly settled to its steady value after forming a breaking crest (see the first frame). No special conditions were applied at the right-hand end of the fluid which collapses like the dam described previously.

For the calculation shown here the viscosity coefficient α was set at 0.1. Smaller values of α result in a turbulent bore,
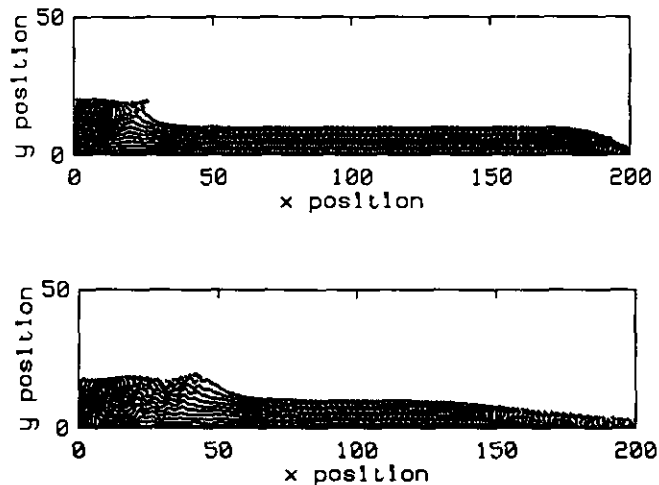

FIG. 3. Particle positions for a viscous bore with fluid travelling from the right to left at 8.5 m/s. The moving fluid meets static fluid with initial depth 20 m. Boundary particles form the base and the barrier to the left. Other details are given in the text.

as expected from both theory and experiment. The theoretical bore speed is 8.6 m/s and the theoretical height of the bore is 20 m. The simulation gives a bore speed of 8.5 m/s with an average height close to 20 m. The density fluctuations were $< 1\%$.

9. WAVE MAKER

This simulation involves a wave maker in the form of an oscillating piston on the left-hand side, a straight-line beach with a slope of 0.1, and a horizontal section 10 m long between the wavemaker and the beach. The SPH simulation used 4552 particles.

The frequency of the oscillation was $1.45\sqrt{g/H}$, where g is the gravitational acceleration, H is the depth of the water at the wave maker (5 m in this simulation), and the amplitude of the wavemaker (the stroke) was 2.5m. For these parameters the deep water wavelength is 14.9 m. Waves with these parameters are expected to spill and produce white water at the crest rather than plunge (*U.S. Army Shore Protection Manual*, Vol. 1), although it is clear that there are no exact criteria for determining what the waves will do.

In Fig. 4 the waves are shown propagating onto the beach. The wavelength is close to the deep water value of 14.9 m, but near the wavemaker the profile of the wave is complicated and only begins to simplify at distances $\gg$ a wavelength [19], but in the simulation this occurs when the effect of the sloping beach begins to be important. The formation of spilling waves is clear, but as the waves evolve they surge.

FIG. 5. Velocity vectors for fluid particles in the last two frames in Fig. 4. Note how the fluid particles move with the piston and note the breaking of the crests.
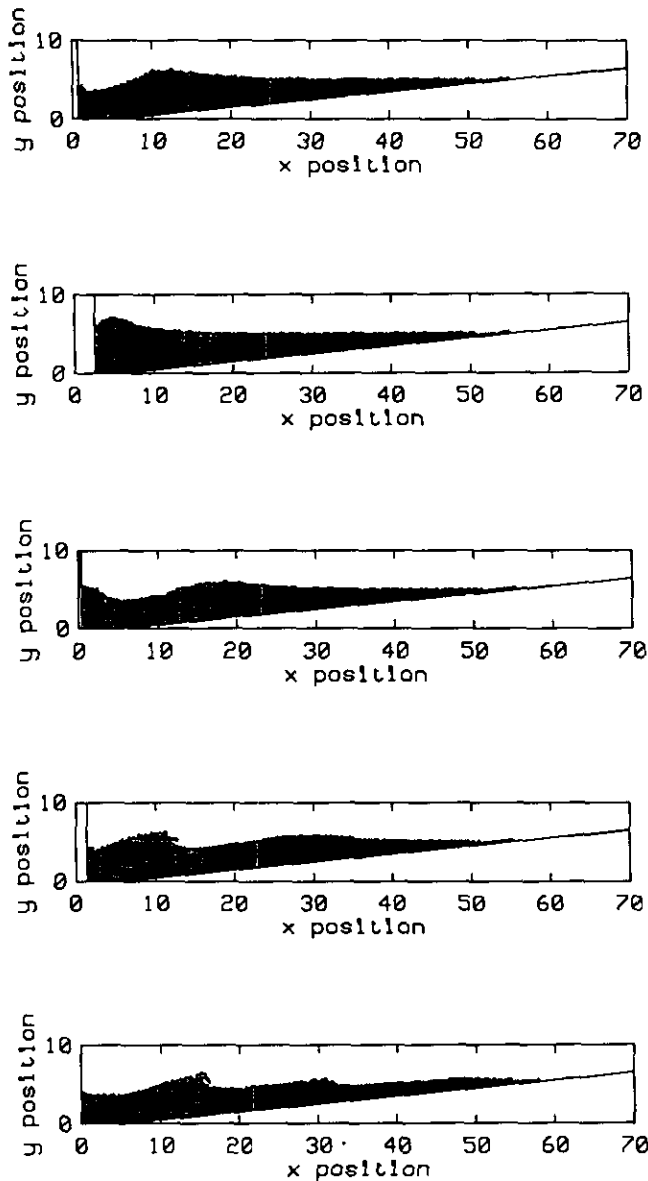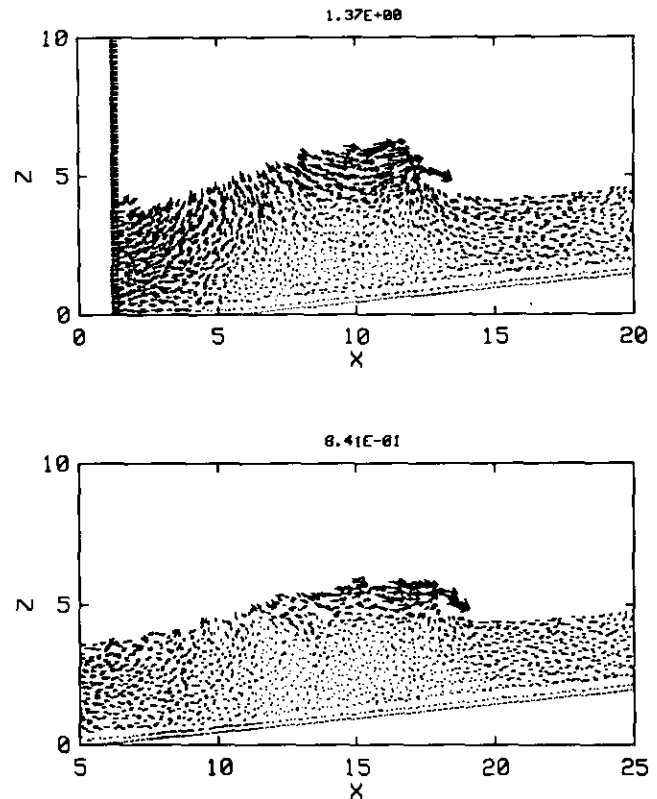

FIG. 4. Particle configurations for the wavemaker. A piston oscillates on the left-hand side. Particles form the bottom boundary and the piston. Details are given in the text.

In Fig. 5 the velocity vectors of the particles for some interesting sections of the waves are shown. Some waves show breaking at the crest, and there is an indication that, with more particles to provide resolution, the crests might plunge. Note that, as in the case of the dam, the particle configuration at the base shows a structure which may be due to discreteness of the boundary. The structure lies within $\sim h$ of the boundary and it takes the form of particles keeping a constant density while decreasing their separation parallel to the boundary and increasing their separation perpendicular to the boundary.

10. DISCUSSION AND CONCLUSIONS

The results of the computations show that SPH can be used to simulate free surface flows without difficulty, provided the density is calculated by approximating its rate of change and the particles are moved with a corrected velocity. The boundary particles give a satisfactory representation of boundaries, but there is evidence from the simulations that the fluid particles note the discreteness of the boundary. It would clearly be useful to optimize the form of the boundary forces because of the great advantages they offer.

The limitation of the use of an artificial equation of state is that the time step is shorter than desirable. Within the present formulation this constraint can only be broken by the development of an implicit scheme. Meanwhile, as emphasized in the Introduction, it remains an advantage of SPH that it provides a simple and reasonably accurate technique for complex problems.

REFERENCES

1. G. K. Batchelor, *An Introduction to Fluid Dynamics* (Cambridge Univ. Press, Cambridge, UK, 1973).

2. W. Benz, *Numerical Modelling of Stellar Pulsation-Nato Workshop* (Les Arcs, France, 1989).

3. R. A. Gingold and J. J. Monaghan, *Mon. Not. R. Astron. Soc.* **181**, 375 (1977).

4. F. Harlow, *Comput. Phys. Commun.* **48**, 1 (1988).

5. F Harlow and J. E. Welch, *Phys. Fluids* **9**, 842 (1965).

6. F. Harlow and A. A. Amsden, *J. Comput. Phys.* **6**, 322 (1970).

7. J. C. Lattanzio, *H.* Pongracic, and M. P. Schwarz, *Mon. Not. R. Astron. Soc.* **215**, 125 (1985).

8. L. Lucy, *Astron. J.* **82**, 1013 (1977).

9. J. C. Martin and W. J. Noyce, *Trans. Phil. Soc.* **244**, 312 (1952).

10. J. J. Monaghan, *Comput. Phys. Commun.* **48**, 89 (1988).

11. J. J. Monaghan, *J. Comput. Phys.* **82**, 1 (1989).

12. J. J. Monaghan, *Annu. Rev. Astron. Astrophy.* (1992).

13. J. J. Monaghan and J. C. Lattanzio, *Astron. Astrophys.* **149**, 135 (1985).

14. B. D. Nichols and C. W. Hirt, *J. Comput. Phys.* **8**, 434 (1971).

15. L. A. Pars, *A Treatise on Analytical Dynamics* (Heinemann, London, 1965).

16. J. Viecelli, *J. Comput. Phys.* **8**, 119 (1971).

17. C. S. Peskin, *J. Comput. Phys.* **25**, 220 (1977).

18. D. Sulsky and J. U. Brackbill, *J. Comput. Phys.* **96**, 339 (1991).

19. T. Havelock, *Phil. Mag.* **8**, 569 (1929).